Spinocerebellar Ataxia Type 1 with Multiple System Degeneration and Glial Cytoplasmic Inclusions

Sid Gilman, MD,* Anders A. F. Sima, MD, PhD,†‡ Larry Junck, MD,* Karen J. Kluin, MS,*§
Robert A. Koeppe, PhD,¶ Mary E. Lohman, BA,* and Roderick Little, PhD**

Spinocerebellar ataxia type 1 (SCA1) is a dominantly inherited progressive neurological disorder characterized by neuronal degeneration and reactive gliosis in the cerebellum, brainstem, spinocerebellar tracts, and dorsal columns. Multiple system atrophy is a sporadic progressive neurological disorder with degeneration and gliosis in the basal ganglia, cerebellum, brainstem, and spinal autonomic nuclei, and with argyrophilic glial cytoplasmic inclusions. We describe 4 members of a family with the SCA1 mutation and a dominantly inherited progressive ataxia in which autopsy examination of 1 member showed neuropathological changes typical of multiple system atrophy, including glial cytoplasmic inclusions. In this patient, magnetic resonance imaging revealed marked brainstem and cerebellar volume loss and mild supratentorial generalized volume loss. Positron emission tomography with [^{18}F]fluorodeoxyglucose revealed widespread hypometabolism in a pattern found in sporadic multiple system atrophy and not in dominantly inherited olivopontocerebellar atrophy. Positron emission tomography with [^{11}C]flumazenil revealed normal benzodiazepine receptor distribution volumes, similar to those seen in sporadic multiple system atrophy. Two other family members still living had similar changes in the imaging studies. The findings in this family suggest that the SCA1 gene mutation can result in a disorder similar to multiple system atrophy, both clinically and neuropathologically.

Gilman S, Sima AAF, Junck L, Kluin KJ, Koeppe RA, Lohman ME, Little R. Spinocerebellar ataxia type 1 with multiple system degeneration and glial cytoplasmic inclusions. Ann Neurol 1996;39:241–255

Olivopontocerebellar atrophy (OPCA) is a progressive neurological disease characterized clinically by cerebellar ataxia and neuropathologically by neuronal degeneration and gliosis in the inferior olives, pons, and cerebellum [1–4]. The disorder occurs sporadically and with hereditary transmission, in both autosomal dominant and autosomal recessive forms. Thus far, genetic studies on patients with dominantly inherited OPCA have identified five independent responsible genetic loci [5–9]. Most patients become symptomatic in middle age with gradually evolving incoordination of gait followed by difficulty with speech and limb movements. Examination reveals ataxia affecting oculomotor, bulbar, and limb musculature and variable involvement of corticobulbar and corticospinal systems, including spasticity of speech and of the limbs, hyperactive muscle stretch reflexes, and extensor plantar responses.

Multiple system atrophy (MSA) is a sporadic progressive neurodegenerative disease manifested clinically by combinations of cerebellar, pyramidal, extrapyramidal, and autonomic symptoms and signs [10, 11]. The neuropathological changes include neuronal loss and gliosis within the inferior olives, pons, cerebellum, substantia nigra, caudate nucleus, putamen, globus pallidus, and intermediolateral columns of the spinal cord [12]. A recently described, distinctive neuropathological feature of MSA consisted of oligodendroglial [13–18] and neuronal [17, 19, 20] intracytoplasmic and intranuclear argyrophilic inclusions containing accumulations to tubular structures. The glial cytoplasmic inclusions (GCIs), which show positive immunostaining for ubiquitin and tau [14, 15], have been detected in striatonigral degeneration (SND), Shy-Drager syndrome (SDS), sporadic olivopontocerebellar atrophy (sOPCA) [21, 22], corticobasal degeneration [23], and hereditary OPCA (in 1 patient) [14]. GCIs were not found in 15 other patients with hereditary OPCA mentioned by Quinn and Marsden [11], 1 patient described by Costa and colleagues [17], or 9 patients

From the Departments of *Neurology, †Pathology, and ‡Internal Medicine; §Division of Speech Pathology, Department of Physical Medicine and Rehabilitation; ¶Division of Nuclear Medicine, Department of Internal Medicine; and **Department of Biostatistics, University of Michigan, Ann Arbor, MI.

Received Feb 17, 1995, and in revised form Aug 4 and Oct 12. Accepted for publication Oct 12, 1995.

Address correspondence to Dr Gilman, Department of Neurology, University of Michigan Medical Center, Taubman Center 1914/0316, 1500 East Medical Center Drive, Ann Arbor, MI 48109-0316.

studied by Abe and coworkers [24]. GCIs were not found in a large number of neurological control subjects, including patients with Parkinson's disease or progressive supranuclear palsy [11].

Although MSA is considered to be a sporadic and not a hereditary disorder, dominantly inherited ataxia at times is associated with neuropathological changes in the basal ganglia, as in OPCA type V of Konigsmark and Weiner [25, 26], and in Machado-Joseph disease [27]. We report here the study of a family with the spinocerebellar ataxia type 1 (SCA1) mutation presenting with a dominantly inherited progressive neurodegenerative disease involving ataxia, dystonia, autonomic dysfunction, and peripheral neuropathy. Clinical neurological, speech, and neuropsychological evaluations were supplemented with anatomical (magnetic resonance imaging [MRI] or computed tomography [CT]) and functional (positron emission tomography [PET]) imaging studies. We compared the functional imaging studies in this family with those obtained from normal control subjects, from patients with sporadic MSA, and from other families with dominantly inherited OPCA (dOPCA).

Materials and Methods

Clinical Evaluations

The studies were approved by the Institutional Review Board, and informed consent was obtained from each subject. The patients were evaluated by questions for medical and neurological histories, physical examinations, neurological examinations, perceptual speech evaluations, neuropsychological testing, MRI or CT, and PET. Testing of blood samples for the SCA1 mutation was performed by a commercial laboratory. Our methods of examining speech in patients with ataxia are described in other publications [28–30].

The neurological disorder in this family was transmitted in a pattern suggesting autosomal dominant inheritance (Fig 1). The disorder affected both males and females, was observed in three successive generations, and was expressed only in the offspring of affected persons. The disease presented clinically with a progressive cerebellar disorder. In 2 patients in their eighth decade (Patients 1 and 2), the cerebellar disorder was associated with impotence, bladder dysfunction, and signs of pyramidal and extrapyramidal dysfunction. Two additional patients in this family had cerebellar disorders beginning in their fifth decade but no symptoms or signs of extrapyramidal or autonomic dysfunction, although both were in an early phase of the disorder. The clinical finding of cerebellar involvement was buttressed by anatomical imaging studies showing both brainstem and cerebellar atrophy (Fig 2). All 4 patients had evidence of mild peripheral neuropathy affecting both sensory and motor fibers.

Positron Emission Tomography

Studies were performed with the subjects lying supine and awake in a quite room, with eyes open and ears unoccluded and alert but not speaking from 5 minutes before injection

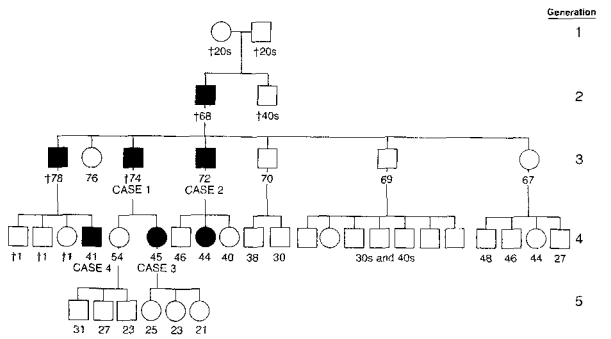

Fig 1. Pedigree showing five generations of the family with the SCA1 mutation. The information in this pedigree was provided by 6 family members in Generations 3 and 4. Filled symbols *indicate affected individuals. Generation 1: Both parents died in their 20s of unknown causes without known neurological disorders. Generation 2: The affected individual developed a cerebellar disorder at age 60 and died of a cerebral hemorrhage at age 68. The sibling died with bronchial asthma and had no neurological disorder. Generation 3: The affected sibling of Patients 1 and 2 developed a cerebellar disorder in his mid-50s and was confined to a wheelchair at the time of death. Generation 4: Three siblings of Patient 4 died between ages 1 and 2 of unknown causes. We did not examine the affected daughter of Patient 2.*

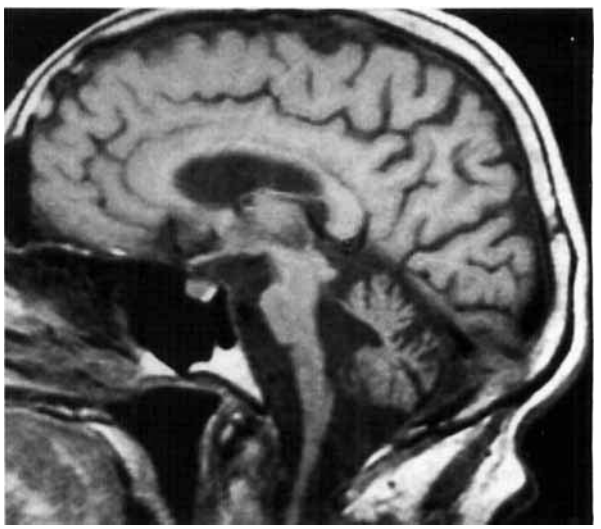

Fig 2. Magnetic resonance image in the sagittal plane of Patient 1, a 72-year-old man, showing cerebellar and brainstem atrophy.

Table 1. Age and Sex Distributions of Subjects Studied with Positron Emission Tomography[a]

		[^{18}F]Fluorodeoxyglucose Studies			[^{11}C]Flumazenil Studies		
	SCA1	dOPCA	MSA	Normal Controls	dOPCA	MSA	Normal Controls
Men	2	10	14	19	6	11	11
Women	1	7	12	32	8	8	9
Total	3	17	26	51	14	19	20
Age (yr, range)	45–72	31–66	47–82	19–76	31–66	44–75	42–82
Age (yr, mean ± SD)	62 ± 15	46 ± 13	63 ± 8	44 ± 17	50 ± 14	63 ± 9	61 ± 10

[a]The 3 patients with the SCA1 mutation were studied with both [^{18}F]fluorodeoxyglucose and [^{11}C]flumazenil. Analysis of covariance was used to adjust for differences in age and sex among the four groups in the data analysis.

SCA1 = patients with the spinocerebellar ataxia type 1 mutation; dOPCA = dominantly inherited olivopontocerebellar atrophy from different families; MSA = multiple system atrophy; SD = standard deviation.

until completion of the scan. The subjects fasted for 4 hours before the PET studies. A catheter was placed in a radial artery for blood sampling. PET scans were performed following intravenous injection of 22 ± 2 mCi of [^{11}C]flumazenil (FMZ) and, 90 minutes later, 10 mCi of [^{18}F]fluorodeoxyglucose (FDG). All subjects were imaged with a Siemens/CTI 931/08-12 scanner, which has an intrinsic in-plane resolution of 5.5-mm full width at half maximum (FWHM) in the center of the field of view and an axial resolution of 7.0-mm FWHM. The reconstructed resolution is 9.0-mm FWHM at the center of the field of view. Fifteen planes with a 6.75-mm center-to-center separation were imaged simultaneously. Attenuation correction was calculated by the standard ellipse method.

The studies with FMZ were performed as a 60-minute sequence of 15 scans and used to measure benzodiazepine (BDZ) receptor density as assessed by ligand distribution volume (DV). The latter is linearly related to the density of available receptor sites divided by the ligand dissociation constant (B_{max}'/K_D). The studies with FMZ also yield regional values for ligand transport (K_1), which is highly correlated with flow since the single-pass extraction fraction for FMZ is greater than 50% [31]. The methods of using FMZ for BDZ receptor binding, including the assumptions, limitations, and performance of the agent, have been published [31–33]. The studies with FDG were performed as two interleaved image sets acquired 30 to 90 minutes after injection, and data were quantified according to the static scan method of Hutchins and associates [34]. Radioactive fiducial markers [31] were used to register all frames of the dynamic FMZ scan and to register the FDG scan to the FMZ scan.

Volume-of-interest (VOI) data were acquired from the cerebral cortex, caudate nucleus, putamen, thalamus, cerebellar hemispheres, cerebellar vermis, and brainstem, as described previously [35]. VOI placement was determined on images of FMZ DV, which provide superb definition of gray matter structures, and the same placement was used on images of FMZ transport (K_1) and local cerebral metabolic rate for glucose (lCMRglc).

DATA ANALYSIS. Data from PET studies with FDG in Patients 1, 2, and 3 in this family were compared with data from 17 patients with dOPCA without known multiple system degeneration from many different families, 26 patients with MSA, and 51 normal control subjects (Table 1). Data from PET studies with FMZ in the same 3 patients in this family were compared with data from 14 patients with dOPCA without known multiple-system degeneration from many different families, 19 patients with MSA, and 20 normal control subjects (see Table 1). Some of the FDG and FMZ data from dOPCA, MSA, and normal control groups have been published [35, 36].

Distributions of three measures—absolute level of lCMRglc, FMZ ligand inflow (K_1), and FMZ DV—were compared in seven regions of the brain. Analysis of covariance was used to adjust for differences in the age and sex distributions of the four groups, and to provide two-sided statistical analyses comparing the means of the study subjects with the means of the dOPCA, MSA, and control groups. When a significant ($p < 0.05$) interaction was found between either age or sex and study group, a separate covariate adjustment for age and sex was applied within each group. Since the comparison groups differed considerably in age, two additional analyses were run restricting all subjects in the comparison groups to (a) all those age 40 or older utilizing adjusted means and (b) all subjects age 45 or older utilizing unadjusted means. A covariance adjustment was not needed for the analysis in (b) since the age means were similar in the four groups. These analyses yielded similar means, suggesting that the covariance adjustments were reasonable.

Histopathology

One patient (Patient 1) was examined neuropathologically. Sections were taken from various cortical areas, anterior and posterior basal ganglia, thalamus, several levels of the brainstem, and cerebellum. They were stained with cresyl violet–Luxol fast blue–eosin (CV-LFB-E), phosphotungstic acid hematoxylin (PTAH), and Bielschowsky's silver stain. Pathological changes, including neuronal loss and gliosis, were scored as follows: 0 = normal; + = mild; ++ = moderate; +++ = severe.

Immunocytochemistry

Paraffin-embedded, 5-μm-thick sections were immunostained with the avidin-biotin-peroxidase complex (ABC)

method [37] with a Vectastain ABC kit (Vector, Burlingame, CA). The following primary antibodies were applied: polyclonal rabbit anti–chicken tau (1:100) (Sigma Chemical, St. Louis, MO); polyclonal rabbit anti–human ubiquitin (1:100) (Dako, Carpenteria, CA); monoclonal phosphorylated neurofilament (1:250) (Sternberger Monoclonals, Baltimore, MD); monoclonal mouse anti–human beta-amyloid (1:100) (Dako, Carpenteria, CA); and polyclonal rabbit anti–human glial fibrillary acidic protein (GFAP) (1:250) (Sigma Chemical, St. Louis, MO).

Nonspecific binding was blocked by pretreatment with a blocking kit (Vector). Negative control samples were performed by omitting the primary or secondary antibody. Sections were incubated with the required primary antibody followed by the secondary reagent, including biotinylated anti–rabbit or anti–mouse IgG for 30 minutes and then with ABC. The sections were then subjected to peroxidase reaction containing freshly prepared 0.02% 3,3' diamino benzidine tetrachloride and 0.05% hydrogen peroxide in 0.05 M Tris–hydrochloric acid buffer at pH 7.6 for 10 minutes at room temperature. Staining was performed on a Histostainer Ig instrument (Leica, Deerfield, IL).

Results

Clinical Summaries

PATIENT 1. The patient was well until the age of 60 years when he progressively had difficulty walking, causing him to fall frequently. At age 64 he experienced dysarthria and then incoordination of his hands, with impaired handwriting. He noted difficulty swallowing solids beginning around the age of 68. His incoordination slowly progressed and he began using a wheelchair consistently by age 69. He denied difficulty with bladder or bowel function, but had been sexually impotent since age 57 or 58. He had non-insulin-dependent diabetes mellitus that was well controlled and hypertension, both of which were detected at age 63. He had a family history of a progressive ataxia affecting at least three generations (see Fig 1).

The most recent physical examination was when the patient was 73 years old, 4 months prior to death, and at that time he was confined to a wheelchair because of severe ataxia of the limbs and trunk. The blood pressure was 140/86 mm Hg while he was sitting. Easily provoked and inappropriate laughter suggested a pseudobulbar affect. Abnormalities of extraocular movements including square-wave jerks on primary gaze, saccadic pursuits, and unsustained nystagmus on lateral gaze were found. Occasionally facial grimaces and involuntary tongue movements appeared. Rapidly alternating tongue movements were moderately impaired. He had a moderately severe mixed dysarthria with ataxic and dystonic components. Moderately severe ataxia was evident in the limbs, with a proximal kinetic tremor on finger-nose-finger testing, and a moderate degree of ataxia on heel-knee-shin testing. Rapidly alternating limb movements were slow and dysrhythmic. Resistance to passive manipulation was normal, even with activation. The deep tendon reflexes were graded at 3 (on a scale of 0–4) except for the ankle reflexes, which were grade 2. The plantar responses were flexor. Sensory examination revealed decreased light touch and pinprick sensations in a stocking distribution in the lower extremities up to the midcalf region. Position and vibration senses were intact. The patient could stand with assistance but was too unsteady to walk. The patient died at age 74 with sepsis and respiratory failure coupled with diabetic ketoacidosis.

Table 2. Neuropsychological Test Results[a] of 3 Patients with the SCA1 Mutation

Patient No.	Age[b] (yr)	Sex	FSIQ	PIQ	MQ
1	72	Male	79	74	80
2	68	Male	79	66	71
3	45	Female	90	87	96

[a]Wechsler Adult Intelligence Scale was used to determine full-scale and performance intelligence quotients; Wechsler Memory Scale, to determine memory quotient.
[b]Age refers to the time of neuropsychological testing.

FSIQ = full-scale intelligence quotient; PIQ = performance intelligence quotient; MQ = memory quotient.

Peripheral nerve conduction studies at age 68 revealed markedly reduced conduction velocities in sensory nerves and moderate slowing in motor nerves with electromyographic evidence of chronic denervation in the muscles of both legs. Neuropsychological testing at age 72 revealed scores at the lower end of the normal range to below normal (Table 2). The patient was not tested for the SCA1 mutation. MRI at age 72 revealed prominent volume loss involving brainstem structures with markedly decreased thickness of the ventral part of the pons, marked thinning of the middle cerebellar peduncles, and decreased transverse dimension of the brainstem at the pontomesencephalic junction; moderate volume loss involving the cerebellar vermis and hemispheres (see Fig 2); and moderate cerebral cortical volume loss for age. Signal intensity within the striatum was normal for age and there was no demonstrable volume loss within the striatum. PET with FDG (Fig 3) and FMZ was performed when the patient was 72 years old.

PATIENT 2. The 71-year-old brother of Patient 1 described lifelong incoordination, with clumsiness in common motor activities, poor skills at sports, and inability to learn to ride a bicycle. He noted increased difficulty with balance and coordination at age 19, causing him to fall frequently. His incoordination progressed very slowly so that he began using a cane for walking at age 63. He required at walker at age 66 and a wheelchair by age 68. At age 54 dysarthria developed and at age 67 he had difficulty swallowing solids when his throat was dry. He had a 17-year history of sexual impotence and a long history of frequency of urination and difficulty emptying the urinary bladder. He complained of diminished memory for about 10 years. The relevant past history included macular degeneration of undetermined cause, cataract surgery bilaterally with lens implantations, and three suicide attempts, each with a medication overdose. The patient did not have diabetes mellitus.

On examination at age 71, the patient was in a wheelchair. The blood pressure was 130/70 mm Hg while he was supine,

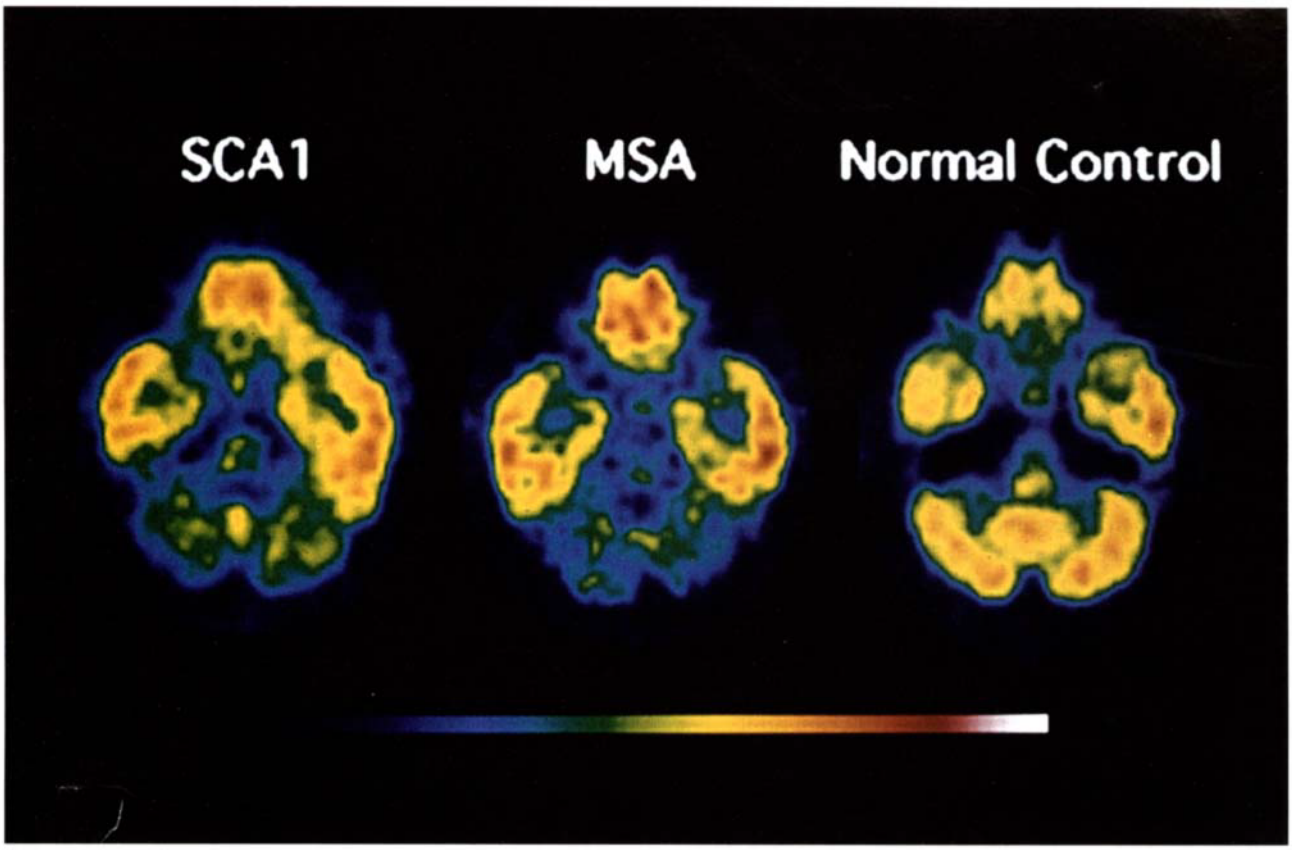

Fig 3. Positron emission tomography scan showing local cerebral metabolic rate for glucose (lCMRglc) as detected with [^{18}F]fluorodeoxyglucose in Patient 1, a 72-year-old man with the SCA1 mutation (left image), *in comparison with scans from a 68-year-old man with multiple system atrophy* (MSA) *whose diagnosis was subsequently confirmed by autopsy examination* (middle image) *and a 74-year-old male, normal control subject* (right image). *The scans show horizontal sections at the level of the cerebellum and the base of the temporal and frontal lobes. The images are normalized to the lCMRglc of the normal control subject. The* color bar *indicates the relative rate of glucose metabolism for all scans illustrated, with colors at the right end of the scale illustrating high rates and at the left end low rates. The scans of the patients with SCA1 and MSA show comparably reduced levels of lCMRglc in the cerebellum and brainstem as compared with the normal control subject.*

declining to 122/68 mm Hg with standing. The pulse remained at 72 beats/min in both the supine and standing positions. Abnormalities of extraocular movements included square-wave jerks, saccadic pursuits, and unsustained nystagmus in the direction of gaze. Both voluntary saccadic and pursuit movements were slow, and overshoot dysmetria occurred. He had a masked face with occasional dystonic facial movements. Rapidly alternating tongue movements were moderately impaired. A moderately severe mixed dysarthria with prominent ataxic components along with some spastic and dystonic elements was detected. Titubation of the head was present when the patient was in the upright position, and alternating flexion-extension and pronation-supination tremors were seen in both hands with the patient at rest, on the left more than the right. Cogwheel rigidity was found at both wrists, but only with activation. Severe ataxia characterized the movements of all extremities and was exhibited on finger-nose-finger and heel-knee-shin tests as well as rapidly alternating movements. The deep tendon reflexes including the ankle reflexes were grade 3 throughout and the plantar responses were extensor bilaterally. The patient was unable to stand unless assisted and could not walk. Sensory testing revealed a stocking-glove distribution of decreased light touch, pinprick, and vibration sensations at the fingers and distal to the calves.

Genetic analysis by a commercial laboratory demonstrated two bands, one with 30 trinucleotide CAG repeats and the second with 43 repeats, indicating that one band was within the affected range of 42 CAG repeats or more. These findings indicate the SCA1 mutation. Peripheral nerve conduction studies at age 69 revealed mild slowing of conduction in both sensory and motor nerves in all four limbs. Electro-

myographic examination revealed minimal abnormal spontaneous activity and an upper motor neuron recruitment pattern. Neuropsychological testing at age 69 revealed scores in the low average range (see Table 2). MRI at age 68 revealed moderate volume loss within brainstem structures, with moderately decreased thickness of the ventral aspect of the pons, moderate thinning of the middle cerebellar peduncles, and decreased transverse dimension of the brainstem at the pontomesencephalic junction; moderate volume loss involving the cerebellar vermis and hemispheres; and mild cerebral cortical volume loss for age. Signal intensity within the striatum was normal for age and there was no demonstrable volume loss within the striatum. PET with FDG and FMZ was performed when the patient was 68 years old. The results are given below.

PATIENT 3. At age 40, the daughter of Patient 1 noted progressively increasing difficulty in walking, frequent falls, and incoordination when driving an automobile. Her gait disorder progressed so that she needed a cane for walking by age 44 and a walker 1 year later. At age 44 dysarthria and intermittent double vision developed and she began complaining of paresthesias in the legs. She had experienced difficulty remembering new information for the previous several years. She complained of occasional difficulty swallowing liquids. The patient did not have diabetes mellitus.

Physical examination at age 47 revealed a blood pressure of 150/90 mm Hg and a pulse of 80 beats/min in the supine position, with no change in the standing position. A pseudobulbar affect was present, manifested by a tendency to laugh and cry easily. Abnormalities of extraocular movements included square-wave jerks, saccadic pursuit movements, and overshoot dysmetria on lateral gaze, but gaze remained conjugate. Dystonic facial expressions were present. Rapidly alternating tongue movements were moderately impaired. She had a moderate mixed dysarthria with prominent ataxic and lesser degrees of spastic and dystonic components. A moderate degree of ataxia was evident on finger-nose-finger and heel-knee-shin testing. The limbs showed normal resistance to passive manipulation, even with activation. The patient could walk only with assistance, manifesting marked unsteadiness. The deep tendon reflexes were all grade 3 except for those at the ankles, which were grade 2. The plantar responses were flexor. Sensory examination revealed decreased vibration sense at the toes bilaterally but no other abnormality.

Genetic analysis revealed one band with 30 CAG repeats and the second with 48 repeats, indicating the SCA1 mutation. Peripheral nerve conduction studies at age 45 revealed moderate slowing of conduction in both sensory and motor nerves in all four limbs. Electromyographic examination revealed a mild degree of abnormal spontaneous activity. Neuropsychological testing at age 45 revealed an average intellect (see Table 2). CT, performed instead of MRI because of claustrophobia, revealed mild thinning of the middle cerebellar peduncles, decreased transverse diameter of the brainstem at the pontomesencephalic junction, moderate cerebellar volume loss, and mild cerebral cortical volume loss. There was no alteration in attenuation or size of the striatum. PET with FDG and FMZ was performed when the patient was 45 years old. The results are given below.

PATIENT 4. This 41-year-old man was the son of an affected brother of Patients 1 and 2 (see Fig 1). Imbalance with walking first developed at about age 30, when he experienced frequent falls. The gait disorder progressed so that by age 37 he began using a walker at home and a wheelchair outside the home. A progressive dysarthria was present for 4 or 5 years. He recently was diagnosed with a bipolar affective disorder. He reported normal sexual function and had no complaints of urinary disorder. He had a history of marked obesity since childhood and at the time of writing weighed about 350 lb.

On physical examination, the blood pressure was 160/90 mm Hg and the pulse was 70 beats/min with the patient in the supine position, and both were unchanged when the patient was upright. Extraocular movements showed no abnormality. A mixed ataxic-spastic dysarthria was detected. A mild degree of ataxia was found on finger-nose-finger testing and a moderate degree on heel-knee-shin testing. The stance was wide and the gait was ataxic with a moderate degree of postural instability. He could not walk on his heels, on his toes, or in tandem. The deep tendon reflexes were grade 3 throughout, but 2 at the ankles. The plantar responses were extensor bilaterally. Sensory examination revealed no abnormalities. An electromyographic and nerve conduction study revealed slowing of nerve conduction velocities compatible with a mild peripheral neuropathy. Anatomical and functional imaging studies were not performed because the patient's body weight exceeded the upper limit allowed.

Positron Emission Tomography

Table 3 summarizes the results of PET studies with FDG for 3 of the patients from the family with the SCA1 mutation in the present study, in comparison to data obtained from patients with dOPCA from multiple different families, MSA patients, and control subjects, adjusted to be comparable with respect to age and sex by analysis of covariance. The mean lCMRglc for the 3 patients was significantly diminished compared with control values in all regions studied: whole brain cortex ($p < 0.05$), caudate nucleus ($p < 0.05$), putamen ($p < 0.05$, two tailed), thalamus ($p < 0.01$), cerebellar hemispheres ($p < 0.001$), cerebellar vermis ($p < 0.001$), and brainstem ($p < 0.001$). The means for the 3 patients were also significantly lower than the means for the dOPCA group for the whole brain cortex ($p < 0.05$), caudate nucleus ($p < 0.05$), putamen ($p < 0.01$), thalamus ($p < 0.01$), and brainstem ($p < 0.05$). The means for the other two regions (cerebellar hemispheres and cerebellar vermis) were also lower than those for the dOPCA group, but these differences were not statistically significant at the 5% level. None of the regional means for the 3 study patients differed significantly from the corresponding means in the MSA group ($p > 0.1$ in all regions).

Table 3. Local Cerebral Metabolic Rates for Glucose (mean ± standard deviation) (mg/100 gm/min) in 3 Family Members with the SCA1 Mutation Compared to 17 Patients with Dominantly Inherited Olivopontocerebellar Atrophy (dOPCA) from Different Families, 26 Patients with Multiple System Atrophy (MSA), and 51 Normal Control Subjects[a]

Structure	SCA1	dOPCA	MSA	Normal Controls
Cerebral cortex	5.52 ± 0.67	7.36 ± 1.16[b]	5.95 ± 1.02	6.58 ± 0.89[b]
Caudate nucleus	6.01 ± 1.37	8.49 ± 1.56[b]	6.93 ± 1.45	7.54 ± 1.30[b]
Putamen	6.47 ± 0.91	9.41 ± 1.45[c]	7.09 ± 1.58	8.32 ± 1.31[b]
Thalamus	6.31 ± 0.68	9.35 ± 1.45[c]	7.36 ± 1.30	8.31 ± 1.20[c]
Cerebellar hemispheres	4.34 ± 0.78	6.07 ± 1.50	4.39 ± 1.19	6.41 ± 0.89[d]
Cerebellar vermis	4.20 ± 0.61	5.49 ± 1.21	4.39 ± 1.07	5.97 ± 0.78[d]
Brainstem	3.97 ± 0.71	5.55 ± 1.05[b]	4.07 ± 0.81	5.72 ± 0.73[d]

[a]Data obtained from dOPCA and MSA patients and the normal control group have been reported previously [35].
[b]Significantly different from SCA1 patients, $p < 0.05$.
[c]Significantly different from SCA1 patients, $p < 0.01$.
[d]Significantly different from SCA1 patients, $p < 0.001$.

Linear discriminant analysis was performed to determine linear combinations of the regional FDG values that best distinguished the MSA, dOPCA, and normal control groups [38]. Data from patients younger than 40 years were excluded from the analysis to limit differences in the age distributions. FDG values from just two regions—the cerebral cortex and the brainstem—were sufficient to account for the differences in the three groups, as the differences by age, sex, and FDG data for the other regions were not significant ($p > 0.1$) after we controlled for these two variables. Figure 4 displays the FDG values of the brainstem and cerebral cortex for the three groups together with the 3 SCA1 patients. Data from Patient 1 are clearly most consistent with membership in the MSA group, and data from the other 2 family members are closer to those for the MSA patients than the dOPCA patients or the normal control group. The linear discriminant analysis yielded estimated probabilities of classification in each group given the values of the variables in the discriminant function, assuming equal prior probabilities. For Patient 1 the estimated probabilities were 0.944 for MSA, 0.051 for dOPCA, and 0.005 for normals. For Patient 2 the estimated probabilities were 0.603 for MSA, 0.265 for dOPCA, and 0.132 for normals. For Patient 3 the estimated probabilities were 0.606 for MSA, 0.326 for dOPCA, and 0.068 for normals.

PET with FMZ in the 3 SCA1 patients revealed K_1 means (Table 4) and DV means (Table 5) that did not differ significantly from the means for the dOPCA, MSA, or normal control groups ($p > 0.05$ for all groups and regions). We reported elsewhere that PET with FMZ revealed diminished ligand influx (K_1) in the cerebellum of patients with dOPCA and in the cerebellum and brainstem of patients with MSA as compared with normal control subjects [36]. These

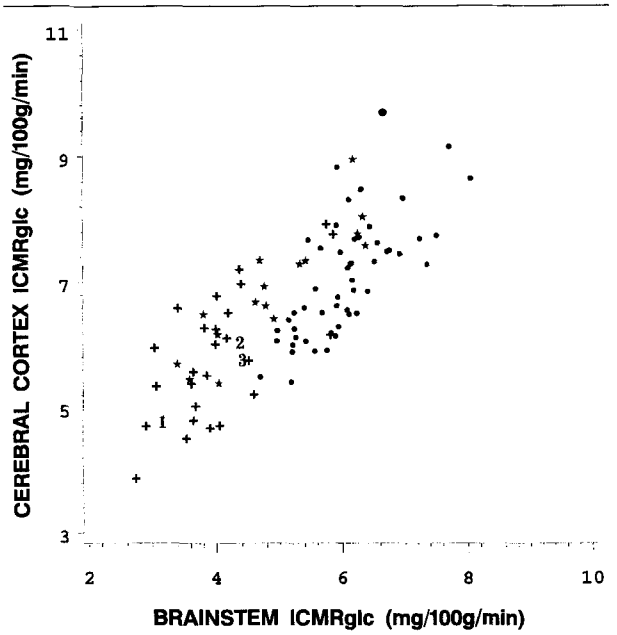

Fig 4. Absolute levels of local cerebral metabolic rates for glucose (lCMRglc) *within the cerebral cortex plotted in comparison with lCMRglc in the brainstem of patients with multiple system atrophy* (crosses), *patients with dominantly inherited olivopontocerebellar atrophy* (stars), *and normal control subjects* (filled circles), *and in the 3 patients with the SCA1 mutation described in this communication (Patients 1, 2, and 3). Data from all 3 patients with the SCA1 mutation are more closely related to the multiple system atrophy patients than to either the dominantly inherited olivopontocerebellar atrophy patients or the normal control subjects.*

Table 4. Flumazenil Influx (K_1)[a] in 3 Family Members with the SCA1 Mutation Compared to 14 Patients with Dominantly Inherited Olivopontocerebellar Atrophy (dOPCA) from Different Families, 19 Patients with Multiple System Atrophy (MSA), and 20 Normal Control Subjects[b]

Structure	SCA1	dOPCA	MSA	Normal Controls
Cerebral cortex	0.34 ± 0.03	0.32 ± 0.06	0.29 ± 0.04	0.29 ± 0.05
Caudate nuclei	0.41 ± 0.01	0.39 ± 0.07	0.37 ± 0.06	0.36 ± 0.06
Putamen	0.45 ± 0.02	0.42 ± 0.08	0.39 ± 0.07	0.38 ± 0.07
Thalamus	0.47 ± 0.003	0.47 ± 0.09	0.46 ± 0.07	0.43 ± 0.10
Cerebellar hemispheres	0.32 ± 0.01	0.34 ± 0.07	0.28 ± 0.08	0.37 ± 0.08
Cerebellar vermis	0.33 ± 0.03	0.32 ± 0.06	0.29 ± 0.08	0.36 ± 0.06
Brainstem	0.28 ± 0.08	0.32 ± 0.06	0.27 ± 0.08	0.34 ± 0.08

[a]Absolute levels in ml/gm/min (mean ± standard deviation).
[b]Data obtained from dOPCA and MSA patients and the normal control group have been reported previously [36].

The findings in the SCA1 group are not significantly different from those in the other two groups ($p > 0.05$). Significant differences in the cerebellar and brainstem structures between dOPCA, MSA, and normal control groups have been reported elsewhere [36].

Table 5. Flumazenil Distribution Volume[a] in 3 Family Members with the SCA1 Mutation Compared to 14 Patients with Dominantly Inherited Olivopontocerebellar Atrophy (dOPCA) from Different Families, 19 Patients with Multiple-System Atrophy (MSA), and 20 Normal Control Subjects[b]

Structure	SCA1	dOPCA	MSA	Normal Controls
Cerebral cortex	5.36 ± 0.89	5.59 ± 0.58	5.48 ± 1.14	5.34 ± 0.90
Caudate nuclei	3.48 ± 0.68	3.07 ± 0.62	3.06 ± 0.66	3.10 ± 0.79
Putamen	3.83 ± 0.28	3.62 ± 0.59	3.92 ± 0.90	3.59 ± 0.64
Thalamus	3.60 ± 0.28	3.73 ± 0.45	3.72 ± 0.76	3.61 ± 0.69
Cerebellar hemispheres	4.67 ± 1.03	4.17 ± 1.07	4.69 ± 1.18	4.21 ± 0.67
Cerebellar vermis	3.94 ± 0.76	3.51 ± 0.81	3.64 ± 0.83	3.66 ± 0.57
Brainstem	1.24 ± 0.06	1.15 ± 0.18	1.14 ± 0.26	1.17 ± 0.18

[a]Absolute levels in ml/gm (mean ± standard deviation).
[b]Data obtained from dOPCA and MSA patients and the normal control group have been reported previously [36].

None of the differences in means between the SCA1 group and the other groups are significant ($p > 0.05$). The results of comparisons between dOPCA, MSA, and normal control groups have been reported elsewhere [36].

studies yielded no evidence of reduced DV in the brainstem, cerebellum, basal ganglia, thalamus, or cerebral cortex in dOPCA or MSA subjects as compared with normal control subjects.

Neuropathological Findings of Patient 1

GROSS EXAMINATION. The brain weighed 1,220 gm. The hemispheres were symmetrical, without gyral atrophy. The cerebral vessels manifested moderate patchy atherosclerosis. The pons and medulla were markedly and symmetrically atrophic, and the midbrain showed moderate atrophy. The cerebellar vermis and hemispheres showed severe atrophy. The brain was bisected and the right hemisphere was fixed in formalin for histopathological examination. The left hemisphere was frozen for biochemical studies.

Coronal sections of the fixed hemisphere revealed normal ventricular size. The cerebral cortex and the centrum semiovale were unremarkable. The head of the caudate nucleus and the lenticular nuclei were mildly atrophic and the caudolateral putamen was discolored. The thalamus and hypothalamus appeared normal. Sectioning of the brainstem revealed moderate pallor of the substantia nigra. The basis pontis and medulla were markedly atrophic. Sectioning of the cerebellum demonstrated atrophy of the cortex and central white matter. The spinal cord appeared unremarkable externally and on sectioning.

MICROSCOPIC EXAMINATION. Sections were stained with CV-LFB-E, PTAH, and Bielschowsky's silver stain and were scored for the severity of the neuronal loss and gliosis (Table 6).

In the medulla, the inferior olivary nucleus showed severe neuronal loss and gliosis (Fig 5A) with axonal loss and pallor of the outflow tract in myelin stains. In the cerebellum, the dentate nucleus exhibited moderate neuronal loss and severe gliosis. The cerebellar hemi-

spheres showed marked loss of Purkinje cells and accompanying Bergman gliosis, mild neuronal loss in the internal granular layer, and pallor of the white matter in myelin stains (Fig 5B). Similiar but milder changes were found in the cerebellar vermis. The pontine nuclei exhibited moderate neuronal loss, marked gliosis, and loss of transverse fibers (Fig 5C). The degenerative changes in the inferior olives, pons, and cerebellum were typical of the findings in OPCA.

In the midbrain, there was neuronal loss and marked gliosis of the periaqueductal gray matter. The oculomotor and trochlear nuclei showed mild to moderate neuronal loss and gliosis, which also affected the Edinger-Westphal nucleus. Similar changes were found in the abducens and facial nuclei in the pons. In the medulla the hypoglossal and vagal nuclei showed mild to moderate neuronal loss and gliosis. The parahypoglossal nuclei exhibited severe neuronal loss and gliosis. The accessory cuneate and ambiguus nuclei were moderately affected.

The substantia nigra exhibited neuronal loss and gliosis of both pars compacta (more pronounced in the lateral part) (Fig 6A) and pars reticularis. The locus ceruleus showed mild neuronal loss and gliosis. Neuronal loss and gliosis were also found in the basal ganglia, most pronounced in the head of the caudate nucleus, globus pallidus, and caudolateral portion of the putamen (Fig 6B). These findings are typical of the changes in striatonigral degeneration.

The thalamus showed neuronal loss and gliosis in the anterior, dorsomedial, and ventroposterolateral nuclear complexes, most severe in the latter.

The lumbar and thoracic spinal cord regions exhibited moderate to severe neuronal loss and gliosis of Clarke's column and the anterior (Fig 7A) and intermediolateral horns (Fig 7B). These changes were associated with mild to moderate axonal loss and pallor of myelin of the cervical dorsal columns and the lateral corticospinal tracts of the lower lumbar region of the cord. Dorsal and ventral spinal roots showed mild to moderate diffuse loss of myelinated fibers. Lumbar dorsal root ganglia displayed moderate loss of ganglion cells with nodules of Nageotte, as well as ganglion cells undergoing cystic degeneration (Fig 7C).

The cortex of the frontal, temporal, parietal, and occipital lobes appeared normal. The hippocampus had occasional neurofibrillary tangles in the CA2 region and a few neuritic plaques were identified in the entorhinal cortex. The nucleus basalis of Meynert was unremarkable. The centrum semiovale appeared normal.

Bielschowsky-stained sections revealed occasional tangle-like inclusions in oligodendroglial cells, similar to the GCIs described by Papp and Lantos and others [13–17, 19–22, 24], in the external and internal capsule, midbrain, pons, medulla, cerebellum, and spinal cord (Fig 8A).

Table 6. Neuropathological Findings[a] of Patient 1

Anatomical Site	Neuronal Loss	Gliosis
Basal ganglia		
Globus pallidus	++	++
Putamen (caudolateral)	++	++
Caudate (head)	++	++
Claustrum	0	+
Thalamus		
Ventroposterolateral	++	+++
Dorsomedial	++	++
Anterior	+	++
Midbrain		
Substantia nigra (compacta)	+	++
Substantia nigra (reticularis)	+	+
Red nucleus	0	+
Periaqueductal gray	++	+++
Oculomotor nucleus	+	++
Trochlear nucleus	++	+++
Edinger-Westphal nucleus	+	+
Pons		
Pontine nuclei	++	+++
Transverse fibers	Axonal loss ++	++
Abducens nucleus	+	+
Facial nucleus	++	++
Locus ceruleus	+	+
Dorsal raphae nucleus	+	+
Medulla		
Inferior olivary nucleus	+++	+++
Hypoglossal nucleus	+	++
Vagal nucleus	++	++
Interpositus	+++	+++
Roller's nucleus	++	++
Ambiguus nucleus	+	++
Accessory cuneate nucleus	++	++
Cerebellar hemisphere		
Purkinje cell layer	+++	++
Granular layer	+	0
White matter	Axonal loss ++	+++
Dentate nucleus	++	+++
Cerebellar vermis		
Purkinje cell layer	++	++
Granular layer	+	0
White matter	Axonal loss +	++
Spinal cord		
Thoracic: Clarke's column	++	+++
Anterior horn	+	++
Intermediolateral column	++	+++
Lumbar: Clarke's column	+++	+++
Anterior horn	++	++
Intermediolateral column	++	+++

[a]Scoring of the severity of neuronal loss and gliosis of involved anatomical systems: 0 = normal; + = mild; ++ = moderate; +++ = severe.

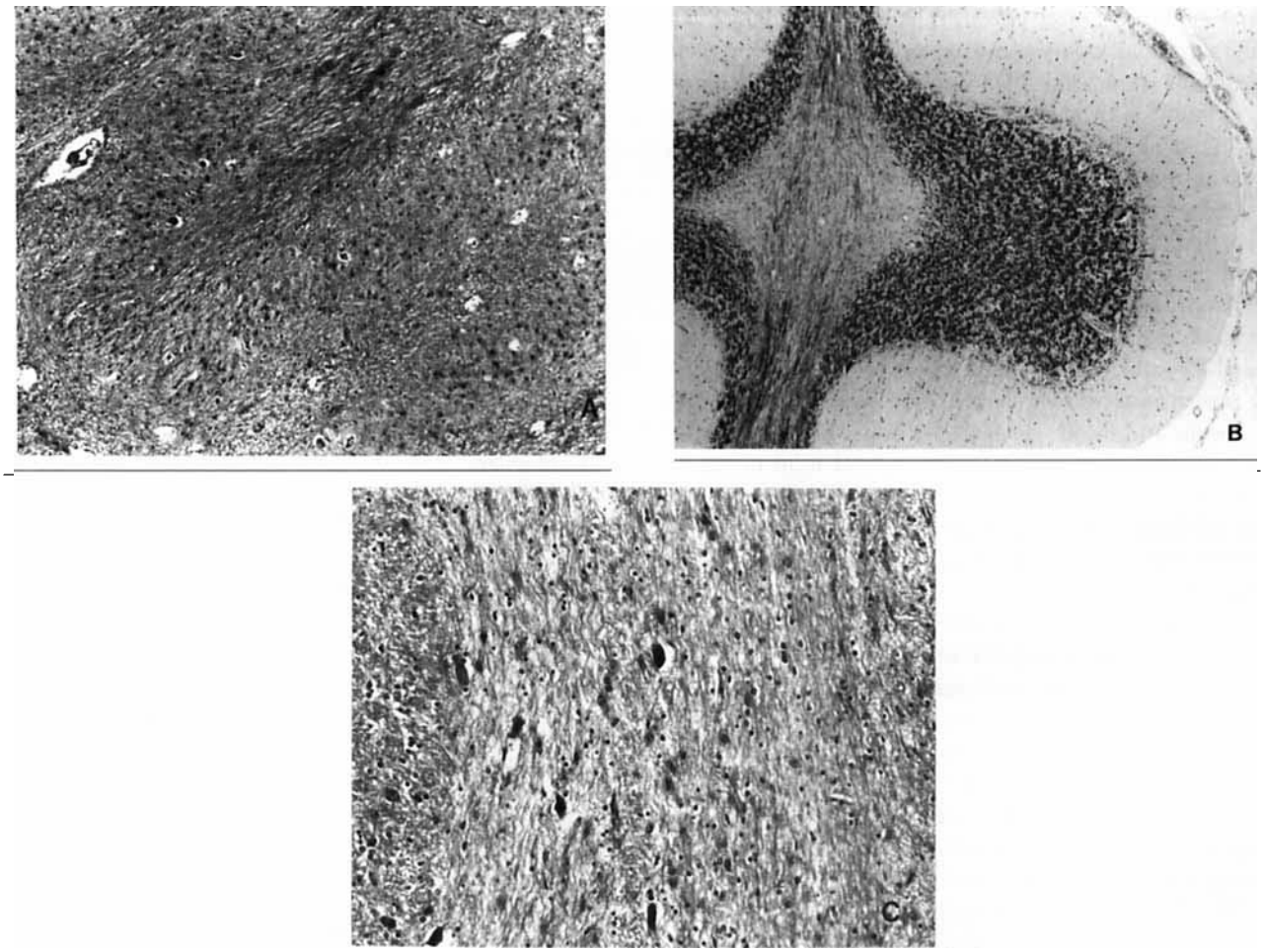

Fig 5. Patient 1. Photomicrographs of the (A) inferior olivary nucleus showing severe neuronal loss and dense astrogliosis (phosphotungstic acid hematoxylin, × 110 before 31% reduction); (B) cerebellum showing marked loss of Purkinje cells with accompanying Bergman gliosis and loss of myelinated fibers (cresyl violet–Luxol fast blue–eosin, × 55 before 32% reduction); and (C) pontine nuclei showing moderate neuronal loss, gliosis, and loss of transverse fibers (phosphotungstic acid hematoxylin, × 560 before 32% reduction).

IMMUNOCYTOCHEMISTRY. The GCIs were most easily identifiable by their positive staining for tau (Fig 8B). They also stained positively for ubiquitin (Fig 8C), but did not stain for phosphorylated neurofilament, beta-amyloid, or GFAP. The GCIs were seen with a frequency of no more than one per 20× field and thus were less common than those found in the MSA patients of Papp and Lantos [20].

Discussion

The patients described here had a dominantly inherited neurodegenerative disease resulting from the SCA1 mutation. The principal clinical features consisted of cerebellar ataxia accompanied by dystonia, autonomic insufficiency, and peripheral neuropathy. The neuropathological changes involved not only the brainstem and cerebellum, as in most patients with the SCA1 disorder, but also the basal ganglia, thalamus, and intermediolateral and ventral columns of the spinal cord. Moreover, the patient evaluated neuropathologically had GCIs, which are currently thought to be an important marker for the diagnosis of MSA [13–17, 19–22]. The distribution of neuropathological changes in the autopsied case was somewhat different from that seen in typical MSA patients, as GCIs were seen in a more limited number than has been described for MSA [13–17, 19–22]. Previously, GCIs were thought to be specific for the diagnosis of MSA; however, tau- and ubiquitin-positive GCIs were recently observed in other disorders, including corticobasal degeneration [23] and chromosome 17–linked dementia [39], and tau-positive tubular astrocytic inclusions were demonstrated in progressive supranuclear palsy [40]. Thus, while GCIs are seen with greatest consistency and frequency in

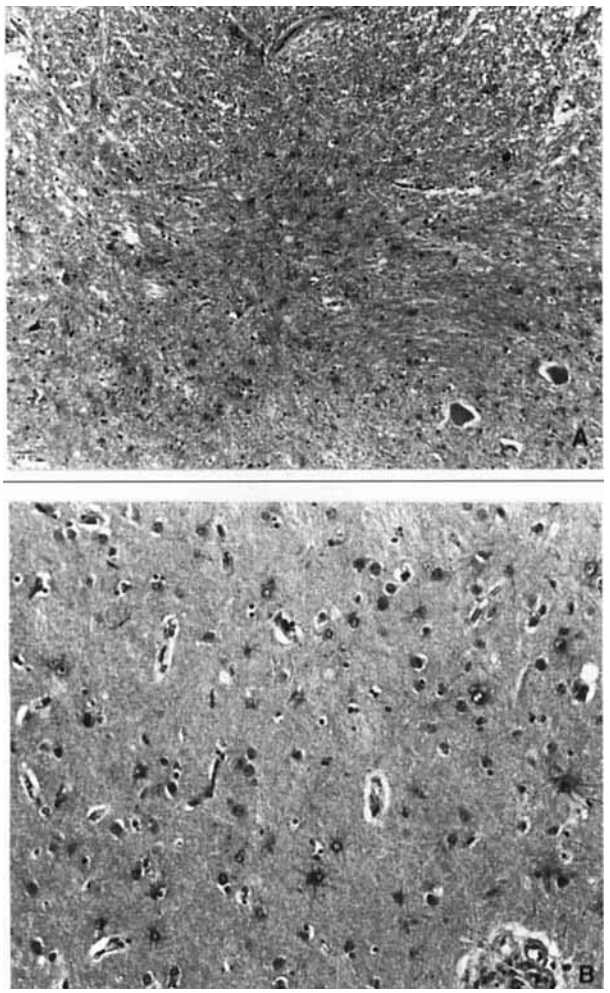

Fig 6. Patient 1. Photomicrographs of the (A) lateral part of substantia nigra pars compacta showing neuronal loss and astrogliosis (phosphotungstic acid hematoxylin, × 280 before 28% reduction) and (B) caudolateral putamen illustrating moderate neuronal loss and gliosis (phosphotungstic acid hematoxylin, × 280 before 27% reduction).

MSA, they are not completely specific for this diagnosis.

Postmortem examinations have been performed on members of several families with the SCA1 disorder [41–46]. The findings typically involve degenerative changes in the cerebellum, brainstem, spinocerebellar pathways, and dorsal columns. Neuronal degeneration often includes the cranial nerve nuclei and anterior horn cells of the spinal cord [45], and the striatum is rarely affected [46]. The extensive involvement of the nervous system seen in the present family, including the basal ganglia, cerebellum, brainstem, and intermediolateral columns of the spinal cord, and the finding of the GCIs have not been described previously.

There may be several reasons for the differences between the patients reported in this communication and other patients reported with the SCA1 mutation. First, the patients in this communication may be similar to others, and further analysis of patients with the SCA1 mutation may disclose autonomic dysfunction, degeneration of autonomic neurons on pathological examination, and GCIs. Second, at least the 2 brothers (Patients 1 and 2) might have a modifying gene that alters the phenotype of these patients. Third, the SCA1 gene may contain a polymorphism that affects the phenotype. Fourth, the phenotype may depend on the number of CAG repeats, though this seems unlikely since in Patient 2 the number of repeats was at the lower end of the abnormal range.

Patients 1 and 2 of the family described here presented clinically with symptoms indicating progressive cerebellar degeneration, later accompanied by autonomic insufficiency. Neurological examination revealed marked cerebellar dysfunction, subtle disturbances of extrapyramidal and pyramidal function, and a long history of sexual impotence. In Patient 1, the sexual impotence could have resulted from a diabetic autonomic neuropathy, but Patient 2 had no evidence of diabetes mellitus and yet had this symptom. The other 2 family members evaluated (Patients 3 and 4) have not as yet shown symptoms or signs of autonomic insufficiency, but they are much younger than Patients 1 and 2. Patient 3 had dystonic facial expressions and dystonic speech components, suggesting an extrapyramidal component to the findings.

The neuropathological changes in Patient 1 included not only the findings of brainstem, cerebellar, and basal ganglia degeneration, but also changes consistent with a sensory and motor neuropathy and a sympathetic and parasympathetic disorder. The clinically and electrophysiologically documented sensory-motor neuropathy in all 4 patients corresponded to the neuropathological changes in Patient 1 of a sensory-motor neuronopathy, with loss of spinal and bulbar motor neurons and dorsal root ganglion cells. In addition, Patient 1 exhibited loss of spinal sympathetic neurons and mild loss of parasympathetic neurons in the Edinger-Westphal nucleus, in keeping with the pathological changes seen in the Shy-Drager form of MSA [18, 47, 48]. These neuropathological changes are not typical of diabetic neuropathy and are likely attributable to the hereditary neurodegenerative disease. Although motor neuron disease is rarely a component of MSA [18], it was reported in one of the original cases of Shy-Drager syndrome [47].

In Patient 1, as typically occurs in MSA, the most severe neuropathological changes in the striatum were found in the caudolateral putamen and the anterior caudate nucleus [10, 12]. Relatively severe degenerative changes were also found in the pallidum and thalamus,

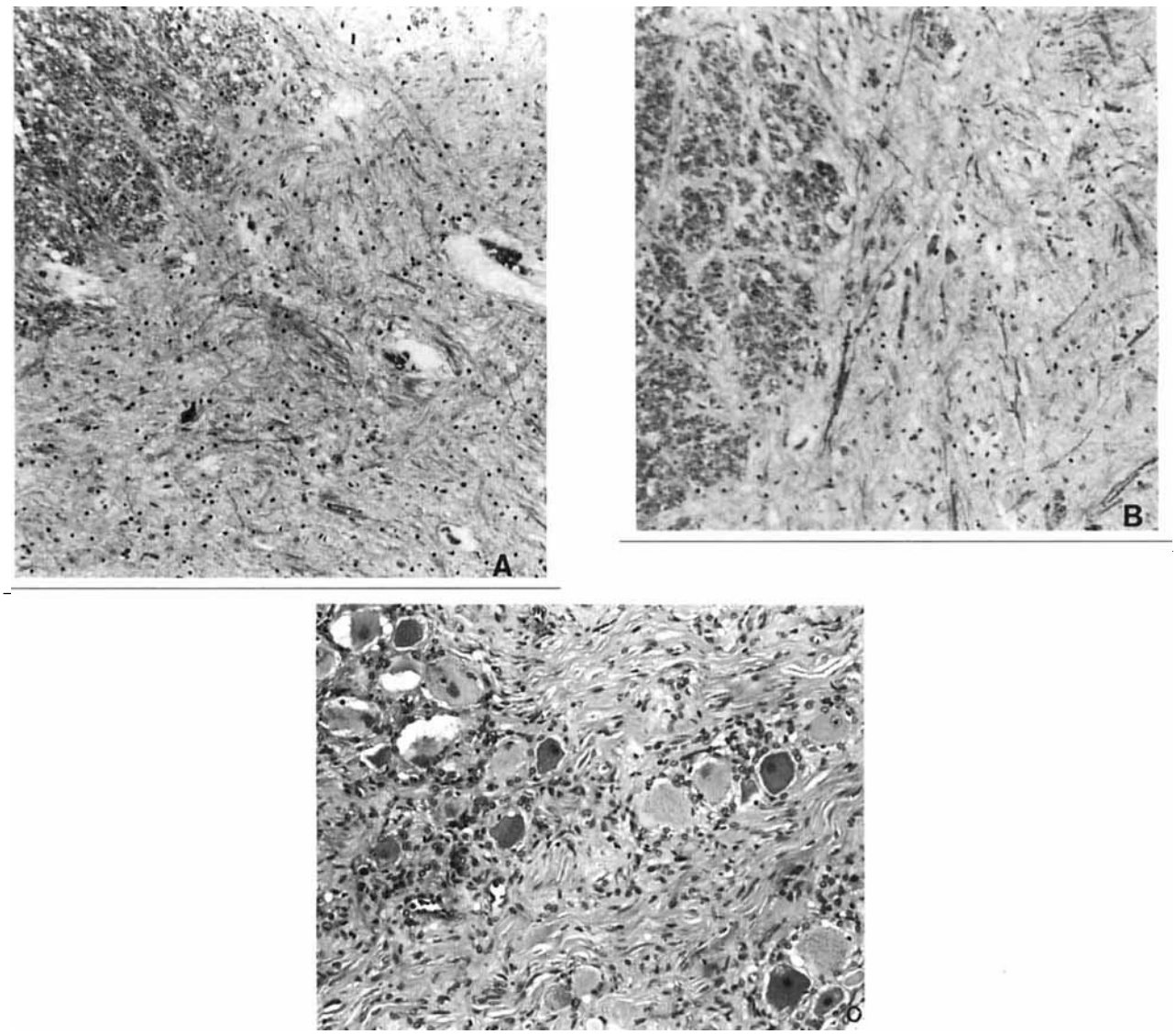

Fig 7. Patient 1. Photomicrographs of the (A) anterior horn of the lumbar region of the spinal cord illustrating loss of motorneurons and isomorphic gliosis, (B) intermediolateral column of the thoracic region of the spinal cord showing loss of sympathetic neurons and gliosis, and (C) lumbar dorsal root ganglion illustrating moderate loss of ganglion cells with nodules of Nageotte and vacuolar degeneration. (Cresyl violet–Luxol fast blue–eosin; A, B: × 280; C: × 560 before 31% reduction.)

and it is not clear whether these changes represent transsynaptic degeneration secondary to changes in the striatum or unrelated degeneration. These structures are usually involved to a lesser extent in MSA. The clinical findings in Patient 2 (the brother of Patient 1) are similar although somewhat milder, suggesting that analogous neuropathological changes are present. At the time of writing, the third affected family member extensively studied remained in the early stages of the disorder, and the clinical studies supplemented by anatomical and functional imaging confirmed the relatively mild degree of impairment.

The clinical findings and anatomical and functional imaging studies partially predicted the marked degenerative changes observed neuropathologically in Patient 1. Atrophy of the brainstem and cerebellum seen by MRI was accompanied by marked glucose hypometabolism in these structures as shown by PET studies with FDG. Despite the moderate severity of neuronal degeneration in the basal ganglia on neuropathological examination, however, the degree of atrophy in anatomical imaging studies was mild. PET with FDG revealed hypometabolism in the cerebral cortex, basal ganglia, and thalamus, and the degree of hypometabolism was similar to that seen in MSA

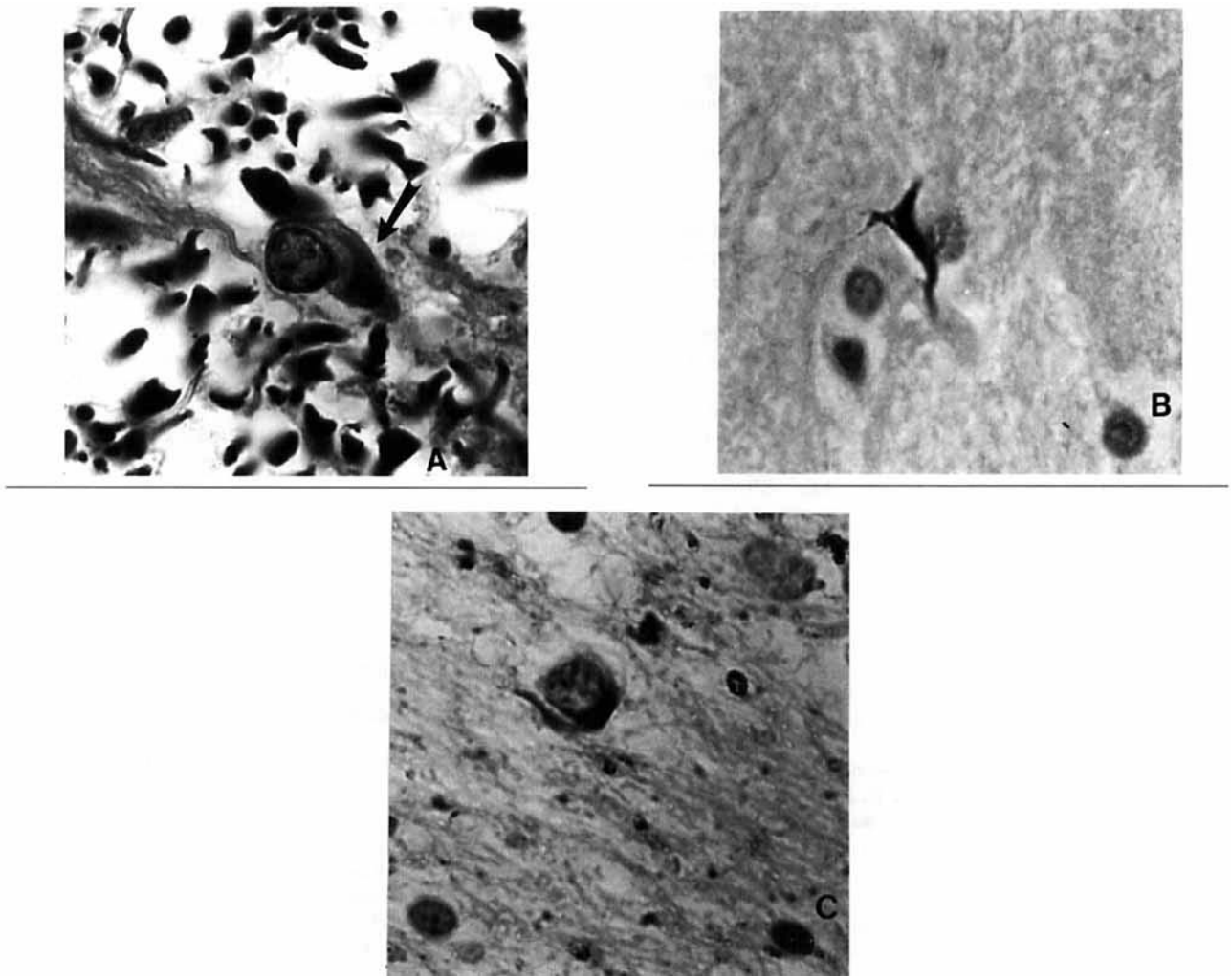

Fig 8. Patient 1. Intracytoplasmic oligodendroglial inclusions in basis pontis stained with Bielschowsky's silver stain (arrow) *(A), in external capsule immunostained with tau (B), and in cerebellum stained with ubiquitin (C). (× 2,240.)*

and much greater than that in dOPCA [35]. The FMZ studies disclosed no important differences in DV between the 3 patients with SCA1 as compared with the dOPCA, MSA, or normal control group, suggesting relative preservation of BDZ receptors. This is in keeping with a recent analysis of FMZ uptake and binding in patients with dOPCA, sOPCA, and MSA [36].

Taken together, the anatomical and particularly the functional imaging studies indicated that the family in this study is different from most families with dOPCA, who do not show evidence of multiple system degeneration. The family shows the distinctive features of multiple system involvement, making it more akin to MSA than to OPCA.

These investigations were supported in part by National Institutes of Health grants NS 15655, NS 24896, AG 08671, and AA 07378.

We thank the personnel of the PET/Cyclotron Center of the Division of Nuclear Medicine for production of the PET isotopes and acquisition of the scans, and Drs David Kuhl and James Brunberg for their assistance.

References

1. Gilman S, Bloedel JR, Lechtenberg R. Disorders of the cerebellum. Philadelphia: Davis, 1981
2. Harding AE. The hereditary ataxias and related disorders. London: Churchill Livingstone, 1984
3. Eadie MJ. Olivo-ponto-cerebellar atrophy (Dejerine-Thomas

type). In: Vinken PJ, Bruyn GW, eds. Handbook of clinical neurology. Amsterdam: North-Holland, 1975:415–431
4. Eadie MJ. Olivo-ponto-cerebellar atrophy (Menzel type). In: Vinken PJ, Bruyn GW, eds. Handbook of clinical neurology. Amsterdam: North-Holland, 1975:433–449
5. Orr H, Chung M-y, Banfi S, et al. Expansion of an unstable trinucleotide (CAG) repeat in spinocerebellar ataxia type 1. Nature Genet 1993;4:221–226
6. Gispert S, Twells R, Orozco G, et al. Chromosomal assignment of the second locus for autosomal dominant cerebellar ataxia (SCA2) to chromosome 12q23-24.1. Nature Genet 1993;4:295–299
7. Matilla T, McCall A, Subramony SH, Zoghbi HY. Molecular and clinical correlations in spinocerebellar ataxia type 3 and Machado-Joseph disease. Ann Neurol 1995;38:68–72
8. Gardner K, Alderson K, Galster B, et al. Autosomal dominant spinocerebellar ataxia: clinical description of a distinct hereditary ataxia and genetic localization to chromosome 16 (SCA4) in Utah kindred. Neurology 1994;44:A361 (Abstract)
9. Ranum LP, Schut LJ, Lundgren JK, et al. Spinocerebellar ataxia type 5 in a family descended from the grandparents of President Lincoln maps to chromosome 11. Nature Genet 1994;8:280–284
10. Quinn N. Multiple system atrophy—the nature of the beast. J Neurol Neurosurg Psychiatry 1989;(special suppl):78–89
11. Quinn N, Marsden CD. The motor disorder of multiple system atrophy. J Neurol Neurosurg Psychiatry 1993;56:1239–1242
12. Daniel SE. The neuropathology and neurochemistry of multiple system atrophy. In: Bannister R, Mathias CJ, eds. Autonomic failure: a textbook of clinical disorders of the autonomic nervous system. Oxford: Oxford University Press, 1992:564–585
13. Papp MI, Khan JE, Lantos PL. Glial cytoplasmic inclusions in the CNS of patients with multiple system atrophy (striatonigral degeneration, olivopontocerebellar atrophy and Shy-Drager syndrome). J Neurol Sci 1989;94:79–100
14. Nakazato Y, Yamazaki H, Hirato J, et al. Oligodendroglial microtubular tangles in olivopontocerebellar atrophy. J Neuropathol Exp Neurol 1990;49:521–530
15. Kato S, Nakamura H, Hirano A, et al. Argyrophilic ubiquinated cytoplasmic inclusions in Leu-7-positive glial cells in olivopontocerebellar atrophy (multiple system atrophy). Acta Neuropathol (Berl) 1991;82:488–493
16. Mochizuki A, Mizusawa H, Ohkoshi N, et al. Argentophilic intracytoplasmic inclusions in multiple system atrophy. J Neurol 1992;239:311–316
17. Costa C, Duykaerts C, Cervera P, Hauw J-J. Les inclusions oligodendrogliales, un marqueur des atrophies multisystématisées. Rev Neurol (Paris) 1992;4:274–280
18. Sima AAF, Caplan M, D'Amato CJ, et al. Fulminant multiple system atrophy in a young adult presenting as motor neuron disease. Neurology 1993;43:2031–2035
19. Kato S, Nakamura H. Cytoplasmic argyrophilic inclusions in neurons of pontine nuclei in patients with olivopontocerebellar atrophy: immunohistochemical and ultrastructural studies. Acta Neuropathol (Berl) 1990;79:584–594
20. Papp MI, Lantos PL. Accumulation of tubular structures in oligodendroglial and neuronal cells as the basic alteration in multiple system atrophy. J Neurol Sci 1992;107:172–182
21. Lantos PL, Papp MI. Cellular pathology of multiple system atrophy: a review. J Neurol Neurosurg Psychiatry 1994;57:129–133
22. Papp MI, Lantos PL. The distribution of oligodendroglial inclusions in multiple system atrophy and its relevance to clinical symptomatology. Brain 1994;117:235–243
23. Wakabayashi K, Oyanagi K, Makifuchi T, et al. Corticobasal degeneration: etiopathological significance of the cytoskeletal alterations. Acta Neuropathol (Berl) 1994;87:545–553
24. Abe H, Yagishita S, Amano N, et al. Argyrophilic glial intracytoplasmic inclusions in multiple system atrophy: immunocytochemical and ultrastructural study. Acta Neuropathol (Berl) 1992;84:274–277
25. Konigsmark BW, Weiner LP. The olivopontocerebellar atrophies: a review. Medicine 1970;49:227–241
26. Woods BT, Schaumburg HH. Nigro-spino-dentatal degeneration with nuclear ophthalmoplegia. J Neurol Sci 1972;17:149–166
27. Coutinho P, Andrade C. Autosomal dominant system degeneration in Portuguese families of the Azores Islands. Neurology 1978;28:703–709
28. Gilman S, Markel DS, Koeppe RA, et al. Cerebellar and brainstem hypometabolism in olivopontocerebellar atrophy detected with positron emission tomography. Ann Neurol 1988;24:223–230
29. Kluin KJ, Gilman S, Markel DS, et al. Speech disorders in olivopontocerebellar atrophy correlate with positron emission tomography findings. Ann Neurol 1988;23:547–554
30. Rosenthal G, Gilman S, Koeppe RA, et al. Motor dysfunction in olivopontocerebellar atrophy is related to cerebral metabolic rate studied with positron emission tomography. Ann Neurol 1988;24:414–419
31. Koeppe RA, Holthoff VA, Frey KA, et al. Compartmental analysis of [^{11}C]flumazenil kinetics for the estimation of ligand transport rate and receptor distribution using positron emission tomography. J Cereb Blood Flow Metab 1991;11:735–744
32. Holthoff VA, Koeppe RA, Frey KA, et al. Differentiation of radioligand delivery and binding in the brain: validation of a two-compartment model for [^{11}C]flumazenil. J Cereb Blood Flow Metab 1991;11:745–752
33. Frey KA, Holthoff VA, Koeppe RA, et al. Parametric in vivo imaging of benzodiazepine receptor distribution in human brain. Ann Neurol 1991;30:663–672
34. Hutchins GD, Holden JE, Koeppe RA, et al. Alternative approach to single-scan estimation of cerebral glucose metabolic rate using glucose analogs, with particular application to ischemia. J Cereb Blood Flow Metab 1984;4:35–40
35. Gilman S, Koeppe RA, Junck L, et al. Patterns of cerebral glucose metabolism detected with positron emission tomography differ in multiple system atrophy and olivopontocerebellar atrophy. Ann Neurol 1994;36:166–175
36. Gilman S, Koeppe RA, Junck L, et al. Benzodiazepine receptor binding in cerebellar degenerations studied with PET. Ann Neurol 1995;38:176–185
37. Hsu S-M, Raine L, Fanger H. Use of avidin-biotin-peroxidase complex (ABC) in immunoperoxidase techniques: a comparison between ABC and unlabeled antibody (PAP) procedures. J Histochem Cytochem 1981;29:577–580
38. Dixon WJ. BMDP statistical software. Berkeley: University of California Press, 1988
39. Sima AAF, D'Amato C, Defendini RF, et al. Primary limbic lobe gliosis; familial and sporadic cases. Brain Pathol 1994;4:538
40. Yamada T, McGeer PL, McGeer EG. Appearance of paired nucleated, tau-positive glia in patients with progressive supranuclear palsy brain tissue. Neurosci Lett 1992;135:99–102
41. Schut JW, Haymaker W. Hereditary ataxia: a pathologic study of five cases of common ancestry. J Neuropathol Clin Neurol 1951;1:183–213

42. Currier RD, Glover G, Jackson JF, Tipton AC. Spinocerebellar ataxia: study of a large kindred. Neurology 1972;22:1040–1043
43. Nino HE, Noreen HJ, Dubey DP, et al. A family with hereditary ataxia: HLA typing. Neurology 1980;30:12–20
44. Bebin EM, Bebin J, Currier RD, et al. Morphometric studies in dominant olivopontocerebellar atrophy. Arch Neurol 1990; 47:188–192
45. Spadaro M, Giunti P, Lulli P, et al. HLA-linked spinocerebellar ataxia: a clinical and genetic study of large Italian kindreds. Acta Neurol Scand 1992;85:257–265
46. Genis D, Matilla T, Volpini V, et al. Clinical, neuropathologic, and genetic studies of a large spinocerebellar ataxia type 1 (SCA1) kindred: $(CAG)_n$ expansion and early premonitory signs and symptoms. Neurology 1995;45:24–30
47. Shy GM, Drager GA. A neurologic syndrome associated with orthostatic hypotension. Arch Neurol 1960;2:511–527
48. Sima AAF, Hoag G, Rozdilsky B. Shy-Drager syndrome: the transitional variant. Clin Neuropathol 1987;6:49–54